Joint Uplink Radio Access and Fronthaul Reception Using MMSE Estimation

Jens Bartelt, Dan Zhang, and Gerhard Fettweis, *Fellow, IEEE*

***Abstract*— In cloud-based radio access networks, remote radio units and central baseband units are connected by fronthaul links, which are commonly assumed to be error-free. However, especially for wireless millimeter wave fronthaul links, this might be challenging to achieve, as they face a more unreliable environment than the conventionally used fiber links. In this paper, we hence aim to mitigate the impact of imperfect fronthaul links. For this, we propose the concept of joint radio access and fronthaul reception, which considers to recover the transmitted messages correctly at the centralized baseband unit, rather than to ensure a nearly perfect fronthaul transmission in between. Based on the Bayesian minimum mean square error criterion, we develop a joint access and fronthaul estimation scheme that can be utilized for various signals transported over the fronthaul, including in-phase/quadrature phase (I/Q) samples, soft-bits, synchronization, and reference signals. In addition, we develop an approximated variant of the scheme to reduced complexity, and an iterative extension to further improve the performance. We demonstrate that our scheme can operate under less reliable fronthaul than conventional approaches by numerical simulation for different signals, and show that our method can be implemented in a parallel architecture to achieve a reasonable computational complexity.**

***Index Terms*— Cloud radio access network, fronthaul, CPRI, MMSE estimation, reliability.**

I. Introduction

TO MEET the ever-increasing traffic demand in mobile networks, the concept of Cloud Radio Access Networks (C-RANs) has been proposed as a future network architecture [1], and has since received a lot of attention both in industry and academia [2]–[4]. By centralizing baseband processing, the C-RAN concept promises increased spectral efficiency by enabling joint processing such as coordinated multi point (CoMP) [5], to increase cost- and energy-efficiency through the utilization of statistical multiplexing and economy of scale, and to reduce the physical size of the radio access points. A detailed study about the current progress and challenges in C-RAN can be found in [4]. One of those challenges is that the C-RAN architecture requires a fronthaul (FH) network to forward baseband samples from remote radio heads (RRHs) to central baseband units (BBUs) and vice versa. Currently, the most widely used FH interface is the Common Public Radio Interface (CPRI) [6]. CPRI employs the forwarding of digitized baseband samples, for which the FH needs to fulfill very challenging requirements. These include a very low latency of a few hundred microseconds, a very high capacity of up to 10 Gbps per cell, and a very high reliability with a bit error rate (BER) of less than 10^{-12}.

The most widely used technology employed for FH today is fiber, as it offers a high data rate due to the large available bandwidth in the optical domain as well as a high reliability. However, a fiber network has to be either deployed by the operators themselves, which requires extensive civil work and the acquisition of rights-of-way, or leased from third parties. Both options can be quite expensive and hence threaten to nullify the cost savings expected from the C-RAN architecture.

Several methods have been proposed to reduce the requirements of the FH in terms of data rate. First, compression schemes have been introduced to reduce the redundancy included in the radio signal of a single cell [7]–[9]. Furthermore, the authors Park *et al.* and Zhou *et al.* have published several works on compression schemes exploiting the correlation among signals from several cells or antennas under a rate limited FH. Overviews of their works can be found in [10] and [11], respectively. Recently, the introduction of different so-called functional splits has received a lot of attention [12]–[16], and is under consideration for standardization, including IEEE 1914.1 Next Generation Fronthaul Interface Working Group [17] and the CPRI consortium's eCPRI standard [6]. The idea behind the functional splits is to perform a part of the baseband processing at the RRHs. The benefit of this is that redundancy embedded in the signals (e.g., guard carriers, cyclic prefix) can be removed before being transported on the FH, and that the different logical channel (e.g., data, reference, synchronization channel) can be either already be processed at the RRH, or forwarded separately.

On the other hand, the use of millimeter wave (mmWave) technologies has been proposed to provide a cheaper and easier to deploy option for FH [15], [18], [19]. While mmWave links cannot cover large distances, the V- and E-Bands, approximately located between 40 and 90 GHz, offer enough bandwidth to transport multi-Gbps data rates and are hence promising candidates for the "last mile" FH in small cell networks. Cost studies have shown that mmWave technology is advantageous compared to fiber in certain scenarios [20].

The main disadvantage of mmWave technology compared to fiber is their lower reliability inherent to their wireless nature.

Manuscript received June 3, 2016; revised November 2, 2016; accepted December 13, 2016. This work is part of a project that has received funding from the European Unions Horizon 2020 research and innovation programme under grant agreement No 671551 (5G-XHaul). The European Union and its agencies are not liable or otherwise responsible for the contents of this document; its content reflects the view of its authors only. The associate editor coordinating the review of this paper and approving it for publication was A. Tajer.

The authors are with the Vodafone Chair Mobile Communications Systems, Technische Universität Dresden, Dresden 01062, Germany (e-mail: jens.bartelt@tu-dresden.de; dan.zhang@tu-dresden.de; gerhard.fettweis@tu-dresden.de).

Color versions of one or more of the figures in this paper are available online at http://ieeexplore.ieee.org.

Digital Object Identifier 10.1109/TCOMM.2016.2644668

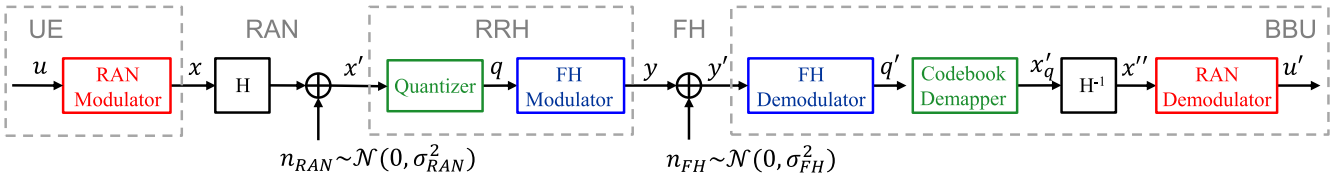

Fig. 1. General system model.

Additionally, mmWave links have to deal with varying channel conditions, as especially the V-band frequencies are severely attenuated by precipitation [21]. Reliability in wireless links is commonly achieved by either using robust modulation and coding schemes (MCSs), or by designing the link budget with a sufficient margin. However, the former increases the complexity in FH transceivers and reduces the effective throughput, while the latter increases energy consumption or limits the maximum achievable range. In this paper, we hence aim to improve uplink performance without having to employ these conventional approaches (although our method can be used in combination with the former two).

The main problem to be addressed in this work is how to recover the original RAN signal received at the RRH from the potentially unreliable FH signal received at the BBU. This introduction of an erroneous FH is in contrast to the above works [1]–[15], which all consider an (almost) error-free FH. The conventional way of designing the fronthaul link is to map the observation of the RAN channel at the RRH into a binary bit sequence which is modulated and forwarded over the FH. The task of the receiver at the BBU link then consists of two stages. During the initial stage, the receiver aims to recover the quantized observation of the RAN channel, while the task of the subsequent stage is to retrieve the information transmitted over the RAN channel. As the quantized observation is used as the true observation for performing the second task, a highly reliable FH link is conventionally required to ensure the performance of the second stage. By enabling joint reception at the centralized BBU, the reliability can be significantly loosened, but this requires an adaption of the receiver. For this, we derive a joint estimation scheme for RAN and FH based on the Bayesian minimum mean square error (MMSE) criterion to produce an MSE-optimal estimate of the original wireless RAN signal by including soft information of the potentially unreliable FH signal.

Several of our earlier works followed similar ideas but were specialized on certain applications. In [22], we proposed a belief propagation method to forward soft information from a FH receiver to the RAN receiver to improve the bit-error rate (BER) in the uplink. In [23], we followed a similar approach but incorporated the more general channel information of the FH BER into the RAN receiver. As we found that the design of the quantizer used for A/D conversion has a very strong impact on the overall performance, this approach was extended in [24] to include a quantizer optimization. All these methods have in common that they include information of the FH signals quality into the estimation of the RAN signal. However, these previous approaches were specifically designed for the data channel of the RAN links, i.e. they focused on improved demodulation and decoding; yet the FH also has to transport other signals like the synchronization channels or reference symbols. Hence, in this work we introduce a more general approach that can be employed for the fronthauling of arbitrary uplink signals. To the best of our knowledge, this principle of joint reception has not been applied to FH networks so far.

The contributions of this work can hence be summarized as follows: 1) we introduce the concept of joint RAN and FH reception, which does not aim for near-perfect FH transmission, but rather targets end-to-end performance, 2) we adopt the Bayesian MMSE criterion to systematically design the joint reception for different types of signals, including I/Q samples, log-likelihood ratios (LLRs), synchronization sequences, and reference symbols, 3) we develop a low-complexity approximation of receiver and an iterative extension for improved performance, 4) we evaluate numerically how the MMSE approach is superior to conventional approaches as it can operate under less reliable FH conditions, and 5) we analyze the computational complexity of the approach and provide an architecture that allows a highly parallel implementation and, while scaling exponentially with the number of quantization bits, requires only linear latency.

The rest of the paper is structured as follows. We will first introduce a system model for a digital FH, and use it to describe the proposed joint reception in comparison to conventional hard-detection, disjoint receivers in Sec. II. We then derive variants for different signals, as well as the reduced-complexity and iterative variants in Sec. III. We will then analyze the performance regarding different metrics and use cases in Sec. IV., and discuss the complexity of the proposed solution in Sec. V. before giving our conclusions in Sec. VI.

II. System Model

To describe the proposed concept, we use a discrete-time baseband model of a single uplink of a mobile network depicted in Fig. 1. We first describe the transmission chain without FH, which will be detailed further below. In general, we denote vectors as $\mathbf{x}$, matrices as X, and their entries as x.[1] $\mathbf{x}_F = \mathfrak{F}(\mathbf{x})$ represents the Fourier transform of $\mathbf{x}$, and $\hat{x}$ an estimate of x. We use $p(\cdot)$ to denote probability distributions, and $\mathrm{E}[\cdot]$ to denote the expected value.

[1]We have skipped indices for the elements of vectors/matrices for the most part of the paper, as we do not require to differentiate between the entries for most signals. The only exception will be the quantization indices described later.

A. Transmitter and Radio Access Channel

In Fig. 1, user data in the form of a bit sequence $\mathbf{u}$ is digitally modulated in the user equipment (UE) to a vector of symbols $\mathbf{x}$ with elements x according to a modulation scheme of order M. The symbols $\mathbf{x}$ are sent over the RAN channel and a distorted version $\mathbf{x}'$ is received. In Fig. 1, the RAN channel is given as an Rayleigh fading channel with additive white Gaussian noise (AWGN), so

$$\mathbf{x}' = H\mathbf{x} + \mathbf{n}_{RAN}, \tag{1}$$

with the entries of H having a Rayleigh-distributed amplitude and uniformly distributed phase, and $n_{RAN} \sim \mathcal{CN}(0, \sigma^2_{RAN})$.[2] Note that we implicitly assume that a cyclic prefix of sufficient length is used, so the frequency domain channel matrix H_F is a diagonal matrix with entries h_F. For H being the identity matrix, the channel becomes an AWGN channel, which will also serve as an illustrative example throughout the paper. However, our receiver is in principle applicable to any channel model as long as the transition probability $p(x'|x)$ is known or can be estimated.

B. Remote Radio Head Processing and Fronthaul Channel

Each of the received symbols x' is analog-to-digital converted by sampling and quantization. As we use a discrete time model, we focus on the quantization. For this, an index q is chosen from a set of indices $q \in I = \{0, \ldots, i, \ldots, 2^B - 1\}$ according to a set of thresholds $\mathcal{T} = \{t_0 = -\infty, t_1, \ldots, t_i, \ldots, t_{2^B-1}, t_{2^B} = \infty\}$:

$$q := i | i \in I,\ t_i \leq x' < t_{i+1}, \tag{2}$$

with B being the quantizer's resolution in bits. Please note that we differentiate in notation between the *current realization* of the index, q, and the general representation of *all possible* indices, i.

For complex-valued symbols, the I- and Q- component are quantized separately. In practice, the codebook indices are digitally represented as a sequence of bits $i = [i_1, \ldots, i_b, \ldots i_B]$ of length B. For each index i there exists an entry from a codebook $\mathcal{C} = \{c_0, \ldots, c_i, c_{2^B-1}\}$, which represents the quantized amplitude value. Thus, the quantized value has three representations: the (decimal) index q, its binary representation $[q_1, \ldots, q_B]$, and its quantized amplitude c_q. Note that while this approach seems to be similar to the well-known scheme of quantize-and-forward (see, e.g. [25]–[27]), our work differs in how quantization is modeled. For quantize-and-forward, a quantizer is represented as a mapping directly from x' to c_q. However, to digitally forward the sample, it needs to be represented by a binary sequence first, which is transmitted over the FH, and is only at the receiver mapped back to its codebook entry. This digital forwarding is used in practical deployments of C-RAN for several reasons. First, the digital forwarding enables the multiplexing of additional data such as monitoring information or control signaling. Second, it can enable a packet-based forwarding, which in turn makes it possible to multiplex several data streams from different RRHs, and to utilize routers and switches for a more flexible FH network. As such, our approach could more appropriately be called "digitize-and-forward".

The design of the quantization codebook is a challenge on its own and several works have focused on optimizing them according to their statistics (e.g., [28], [29]). However, uniform and linear codebooks are commonly used in practice, as they are easier to implement, and because a real-time optimization according to signal statistics is difficult to employ in practice. Nevertheless, our work is applicable to any form of codebook.

The bit sequence $[q_1, \ldots, q_B]$ is next digitally modulated for FH transmission to one or multiple symbols y and sent over the wireless FH channel and received as y'. Please note that, according to the quantizer resolution B and the modulation scheme used on the FH, each bit sequence can be modulated to one or multiple symbols y. Hence, we write y_b to indicate the symbol resulting from the modulation of the b-th bit of q. In Fig. 1 we use an AWGN channel as an example, for which the received FH symbols are given as $y' = y + n_{FH}$ with $n_{FH} \sim \mathcal{CN}(0, \sigma^2_{FH})$. Similar to the RAN channel, any other channel model can be applied if the transition probability $p(y'|y)$ is known or can be estimated. However, both for fiber and mmWave FH links, AWGN is an appropriate model in most cases, as both are static setups and mmWave FH links are usually line of sight links with almost no multi-path propagation due to the highly directive antennas required to overcome the high pathloss.

C. Conventional Baseband Unit Processing

In the following, we first describe the conventional FH receiver before introducing our proposed MMSE receiver in the next section. Conventional systems use an ad-hoc approach of simply reversing the processing performed at the transmitter to recover the sample amplitudes. The received FH symbols y'_b can be soft demodulated by calculating the log-likelihood ratios (LLRs) based on conditional probabilities:

$$L(q_b) = \log\left(\frac{p(q_b = 0|y'_b)}{p(q_b = 1|y'_b)}\right) \tag{3}$$

$$= \log\left(\frac{p(y'_b|q_b = 0)}{p(y'_b|q_b = 1)}\right) \quad \text{if} \quad p(q_b = 0) = p(q_b = 1) \tag{4}$$

However, based on the values of L, hard decisions have to be made to reconstruct the codebook index q'. This index is demapped according to the codebook $\mathcal{C}$ to reconstruct the amplitudes $\tilde{x} := c_{q'}$. These amplitudes ideally should correspond to the amplitudes x' received at the RRH. However, they are distorted both by quantization noise and bit flips between q and q' caused by the FH transmission. These additional bit-flips are not considered in conventional receivers and give rise in the joint receiver that will be discussed later.

Next, we assume that a part of the symbols $\mathbf{x}$ are used as reference symbols that are known at the receiver. The channel is hence at the receiver estimated from these reference symbols using frequency domain channel

[2]Note that this can be easily extended to include inter-symbol interference by making x a vector and h a (channel-) matrix.

estimation:

$$\hat{H}_F = \left(\operatorname{diag}(\mathbf{x}_F^H) \operatorname{diag} \mathbf{x}_F + \frac{\sigma^2_{\mathrm{RAN}}}{\mathrm{E}[h^2]} \mathrm{I} \right)^{-1} \operatorname{diag}(\tilde{\mathbf{x}}_F^H) \operatorname{diag}(\tilde{\mathbf{x}}_F) \tag{5}$$

We assume that the reference symbols are being sent time-multiplexed in a block with the data symbols $\mathbf{x}$, where half of the symbols are reference symbols, and that the channel is constant for the duration of the whole block.

Next, the signal is equalized, e.g. using a frequency-domain MMSE equalizer:

$$\mathbf{x}'' = \mathfrak{F}^{-1} \left(\left(\hat{H}_F^H \hat{H}_F + \frac{\sigma^2_{RAN}}{\mathrm{E}[x^2]} I \right)^{-1} \hat{H}_F^H \tilde{\mathbf{x}}_F \right), \tag{6}$$

with I being the identity matrix. In case of multiple receive antennas, the signal from each antenna is equalized separately and then equal gain combining is utilized to combine the separate streams into a single signal. The amplitudes x'' are finally soft demodulated to receive the user bits u'.

III. A Joint Access and Fronthaul MMSE Receiver

As mentioned above, the conventional method does not consider any FH errors and hence works well when the FH can be made (nearly) error-free; however, as explained in the introduction this comes at a considerable cost in energy, complexity, or coding overhead. Also, the ultimate goal is not to make the FH error-free, but to ensure end-to-end performance. Hence, any distortion of the FH channel can be seen as part of the joint end-to-end channel. Since the RAN receiver is already designed to deal with distortions on the RAN channel, the same mechanisms can be applied to a joint RAN/ FH channel. However, this requires an adaption of the receiver in order to consider the specific structure of the joint RAN/ FH channel, and to be able to forward reliability information on the FH. The conventional method described above processes the FH and RAN signals disjointly, although the former is basically a digital representation of the latter, thereby introducing two disadvantages. First, the soft demodulation of the FH signal y' gives us reliability information on the bits of q' in form of the conditional probabilities $p(q_b|y'_b)$. However, this soft information is discarded, because the codebook demapping requires a hard-defined bit sequence q' to be demapped to an amplitude $\tilde{x} = c_{q'}$. Discarding the soft information on q' can be expected to lead to a degradation and it would therefore be beneficial to preserve it in some way. Second, the soft demodulation of any symbol in general and of y' in particular typically assumes an equal distribution of the bits 0 and 1 as indicated in Eq. (4). However, when using a uniform linear quantizer, the distribution of the indexes q will follow the distribution of x', which for most RAN channels will not be uniform (e.g., Gaussian for an AWGN/Rayleigh channels). As the distribution of x' can either be calculated based on general parameters like the SNR, or can be measured, this information should also help to improve performance.

To exploit these properties, we combine the demodulation of the FH and the codebook demapping into one joint estimation step, which is depicted in Fig. 2. We produce a weighted average of all possible codebook indices, with the weights being derived from the FH channel transition probabilities. This follows the Bayesian principle of the minimum mean square error estimator (see, e.g., [30]) to minimize the difference between the originally received signal x' and its version after the FH transmission $\tilde{x}$, i.e. $\mathrm{E}\left[(x' - \tilde{x})^2 | y'\right]$. We chose the MSE as optimization metric as we want to utilize the same joint receiver not only for encoded user data, but also for synchronization sequences and references symbols used for channel estimation. For these, we consider the MSE to be an appropriately universal metric. For the MMSE estimator, we have derived several variants, which differ either in the complexity involved, or the use case. These variants are discussed in the following subsections.

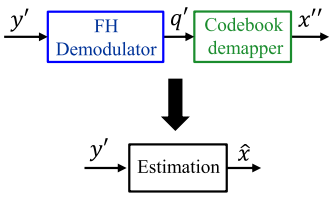

Fig. 2. Advanced receiver that combines the soft information of the FH receiver with the codebook demapping.

A. General Variant

Following the general result for the Bayesian MMSE estimator [30], we can calculate an estimated symbol $\hat{x}$ as:

$$\begin{aligned}
\hat{x} &= \arg\min_{\tilde{x}} \mathrm{E}\left[(x' - \tilde{x})^2 | y'\right] && (7)\\
&= \mathrm{E}[x'|y'] && (8)\\
&= \int_{x'} x' p(x'|y')\, dx' && (9)\\
&= \int_{x'} x' \frac{p(x')p(y'|x')}{p(y')}\, dx' && (10)\\
&= \frac{\int_{x'} x' p(x') p(y'|x')\, dx'}{\int_{x'} p(x') p(y'|x')\, dx'} && (11)\\
&= \frac{\int_{x'} x' \sum_x p(x) p(x'|x) p(y'|x')\, dx'}{\int_{x'} \sum_x p(x) p(x'|x) p(y'|x')\, dx'} && (12)\\
&= \frac{\int_{x'} x' \sum_x p(x) p(x'|x) \prod_b p(y'_b|q_b)\, dx'}{\int_{x'} \sum_x p(x) p(x'|x) \prod_b p(y'_b|q_b)\, dx'}. && (13)
\end{aligned}$$

Eq. (8) is the Bayesian MMSE estimator according to [30], Eq. (9) is the definition of the expected value, Eq. (10) results from Bayes' theorem, Eq. (11) and Eq. (12) result from the law of total probabilities, and Eq. (13) results from the fact that all bits q_b of a codebook index q at the quantizer output are independently modulated and transmitted. The probabilities $p(x'|x)$ and $p(y'_b|q_b)$ represent the channel transition probabilities and depend on the RAN and FH channel models, as well as on the used modulation scheme. By making use of this joint RAN/ FH estimation, the proposed receiver can operate at a lower FH SNR, i.e. reliability, which will be discussed in Sec. IV.

The calculations above face the practical challenge of evaluating integrals over channel transition probabilities in

real time. An example for the closed-form integral of an AWGN channel is given in the appendix. However, the integrals might not be available in closed form or the channel model might not be known at all. Hence, to mitigate the complexity of the implementation, a simplified version can be utilized, which is described in the next subsection.

B. Simplified Variant

Instead of calculating the expected value of the continuous output of the RAN channel x', we can calculate the expected value of the quantized version of it, following similar derivations as in Eqs. (9)-(12):

$$\hat{x} = \mathrm{E}[c_q|y'] = \sum_{i=0}^{2^B-1} c_i\, p(q=i|y') \tag{14}$$

$$= \sum_{i=0}^{2^B-1} c_i \frac{p(i)p(y'|i)}{p(y')} \tag{15}$$

$$= \frac{\sum_{i=0}^{2^B-1} c_i\, p(i)p(y'|i)}{\sum_i p(i)p(y'|i)} \tag{16}$$

$$= \frac{\sum_{i=0}^{2^B-1} c_i\, p(i)\prod_b p(y'_b|i_b)}{\sum_i p(i)\prod_b p(y'_b|i_b)}, \tag{17}$$

with

$$p(i) = \int_{t_i}^{t_{i+1}} p(x')\,dx' = \sum_x p(x) \int_{t_i}^{t_{i+1}} p(x'|x)dx'. \tag{18}$$

As can be seen, the main difference to the general variant is that the integrals have been replaced with sums over all possible quantizer outputs. The latter equation again requires the evaluation of an integral. To further simplify the scheme, the probability $p(i)$ can simply be *observed* at the RRH, i.e. by counting the occurrences of each i over a time interval in which the channel can be expected to be constant (e.g., over the channel's coherence time) and forwarding this information along with the data signal. This also removes the need to know an exact model for the RAN channel. Knowledge of the FH channel is still required for the calculation of $p(y'_b|i_b)$. From the equations above we can see now that – as we mentioned earlier – any model can be applied for both channels as long as the transition probabilities $p(x'|x)$ and $p(y'_b|i_b)$ are known or can be measured, which makes the approach quite versatile. Exemplary closed-form equations for the case of AWGN and Rayleigh channels are given in the appendix. We would like to note that the proposed receiver can also operate in combinations with an encoded FH. In that case, the FH transition probabilities would be provided by a soft-output FH decoder.

To illustrate the difference between the joint receiver and a conventional disjoint receiver, Fig. 3 shows the probability density functions (PDFs)[3] of x', the digitized version c_q, the conventional, hard-decision $\tilde{x} = c_{q'}$, and the improved $\hat{x}$ for a 4 bit quantizer, and an AWGN FH channel with

[3]Pleas not that the discrete variable c_q and $\tilde{x}$ in fact exhibit probability mass functions (PMFs). For better illustration the PDFs have been scaled to approximately match the PMFs.

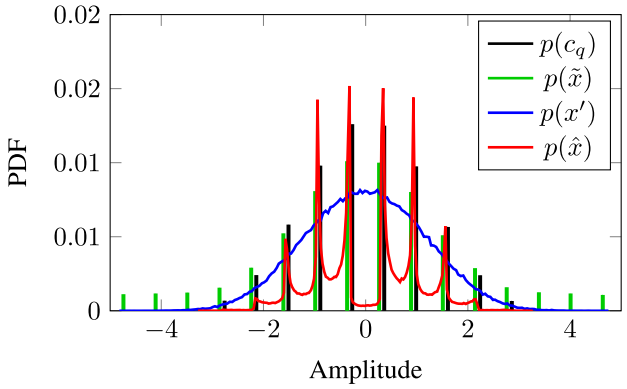

(a) Rayleigh RAN channel.

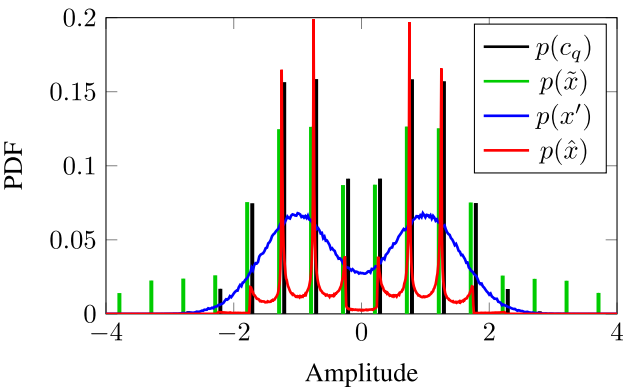

(b) AWGN RAN channel.

Fig. 3. PDFs of different signals: the received symbols at the RRH (x', blue), their digitized representation (c_q, black), the received symbols after the FH using a conventional receiver ($\tilde{x} = c_{q'}$, green) and the proposed receiver ($\hat{x}$, red).

$\mathrm{SNR}_{\mathrm{FH}} = 3$ dB. Fig. 3a gives the distributions for a Rayleigh RAN, and Fig. 3b for an AWGN RAN channel, both with $\mathrm{SNR}_{\mathrm{RAN}} = 5$ dB. The distribution $p(x)$ are of (bimodal) Gaussian shape, with the distribution of c_q being a discretized version of them. The distribution of $p(\tilde{x})$ is also discrete, and additionally exhibits some characteristic side-lobes. These side-lobes are a results of bit flips between q and q', which shift the main lobes around ± 1. A more detailed discussion on this can be found in [24]. The distribution $p(\hat{x})$ also exhibits peaks at the values of $\mathcal{C}$. However, they are smoothed and the side-lobes are visibly suppressed by including the knowledge the original distribution of x'.

C. Soft-Bit Variant

As described in the introduction, it can be beneficial for C-RAN networks to perform a part of the baseband processing already at the RRH to reduce the FH requirements [12]–[16]. One option for this is to perform all steps up unto demodulation at the RRH. In this case, quantized soft-bits instead of amplitude values are transmitted over the FH. Our baseband model can be modified to reflect this by moving the RAN demodulator to the RRH in front of the quantizer as depicted in Fig. 4. The soft-bits are defined as:

$$\lambda(x') = \tanh\left(\frac{1}{2}\log\left(\frac{p(x'|x=-1)}{p(x'|x=+1)}\right)\right). \tag{19}$$

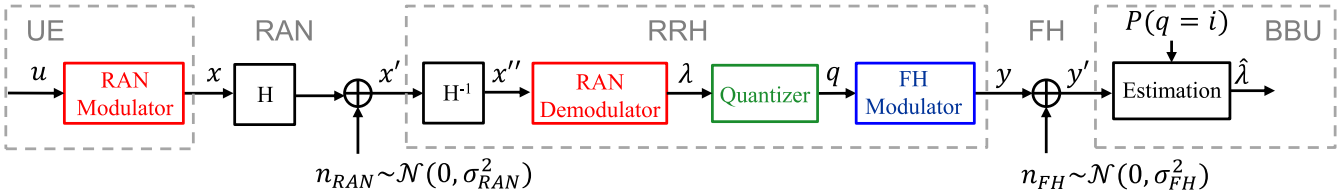

Fig. 4. System model for soft-bit fronthauling with exemplary AWGN channels.

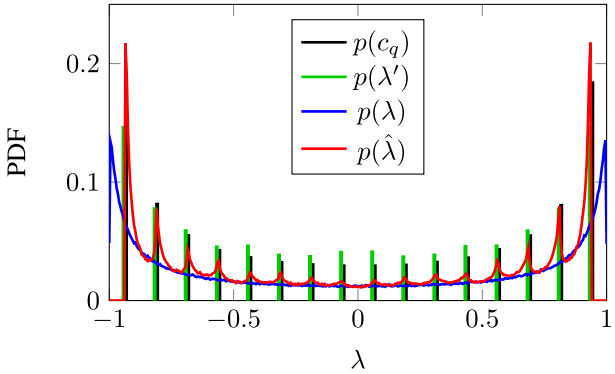

Fig. 5. PDFs of different signals for soft-bit fronthauling: the soft-bits at the RRH (λ, blue), their digitized representation (c_q, black), the soft-bits symbols after the FH using a conventional receiver ($\lambda' = c_{q'}$, green) and the proposed receiver ($\hat{\lambda}$, red).

The probabilities $p(x'|x)$ are typically calculated by the demodulator assuming a Gaussian distribution of x', i.e. an AWGN channel. Eq. (17) can now be applied to the soft-bit signal without modification with $\hat{\lambda}$ replacing $\hat{x}$. The difference is that a different codebook $\mathcal{C}$ will be used as λ is always bounded by $[-1, +1]$, and that the distribution of the quantizer output is now given as:

$$p(i) = \int_{t_i}^{t_{i+1}} p(\lambda')\, d\lambda = \sum_x p(x) \int_{t_i}^{t_{i+1}} p(\lambda'|x)\, d\lambda. \quad (20)$$

A closed-form equation for AWGN channels and BPSK modulation is given in the appendix. Fig. 5 shows the distribution of c_q, λ, λ' and $\hat{\lambda}$ for an AWGN channel and BPSK modulation. Similar to Fig. 3, the distribution $p(\hat{\lambda})$ is a smoothed version of the discrete distribution $p(\lambda')$. After the estimation at the BBU receiver, the soft-bits $\hat{\lambda}$ can be fed into a soft-input decoder for further processing.

D. Iterative Variant: Feedback From the Decoder

The calculation in Eq. (13) and Eq. (18) contain the a-priori information of $p(x)$. Usually, we can assume that all modulation symbols are equally distributed, i.e. $p(x) = 1/M$. However, we can also utilize this a-priori information for an iterative scheme in connection with a soft decoder to further improve performance, which is depicted in Fig. 6. Soft-output decoders (see, e.g., [31]) calculate both the probabilities for each of the original bits and for the encoded bits u. As we are usually interested in the original bits, the information of the encoded bits is usually not used. However, we can utilize the bit probabilities in a soft symbol mapper and feed the resulting symbol probabilities back into the receiver to use

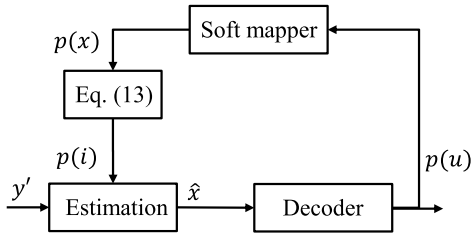

Fig. 6. Iterative variant: the decoder soft-output is fed forward to modify the distribution $p(i)$.

as a-priori information for $p(x)$. Thus, instead of using the *expected* probabilities $p(x)$, we can use the decoder result to have an a-priori probability *for each individual symbol* x. With this new information, the MMSE symbol calculation can be performed again and the soft-symbols again decoded. This process can be iterated for several times to improve reliability. As we will show in Sec. IV-C, these iterations can further increase performance. However, it can be used only in combination with encoded bit data, i.e. not for synchronization or reference signals. In addition, the iterative approach is not directly applicable to the Rayleigh RAN channel, as for this case the distribution $p(x'|x)$ is similar for all x due to the random phase rotation (compare Fig. 3). Hence, the weighting with $p(x)$ does not provide benefits.

IV. Performance Evaluation

In this section, we look at the improvements that the proposed joint receiver and its variants offer compared to the conventional, disjoint scheme. This will include the MSE, the mutual information, end-to-end BERs, the missed detection probability on a synchronization channel, and the channel estimation error.

To obtain theoretic results for all of these metrics, it would be necessary to calculate probability distribution parameterized by $\hat{x}$ in some form (see e.g. $p(\hat{x}|x)$ in Eq. (21)). However, we found this to be analytically intractable, as the sum in Eq. (17) leads to a convolution of distributions, and the product leads to a distribution that requires the evaluation of the Meyer-G-function [32], [33], which can only be evaluated numerically. Therefore, we evaluate all metrics in this section by means of Monte-Carlo simulation.

A. Mean Square Error (MSE)

We first discuss the impact of the proposed scheme on the MSE, which the Bayesian approach is intended to minimize. Fig. 7 shows the MSE for AWGN RAN and FH channels of different SNRs. Clearly, the MMSE receiver exhibits a lower MSE for all values, or – conversely – offers the same

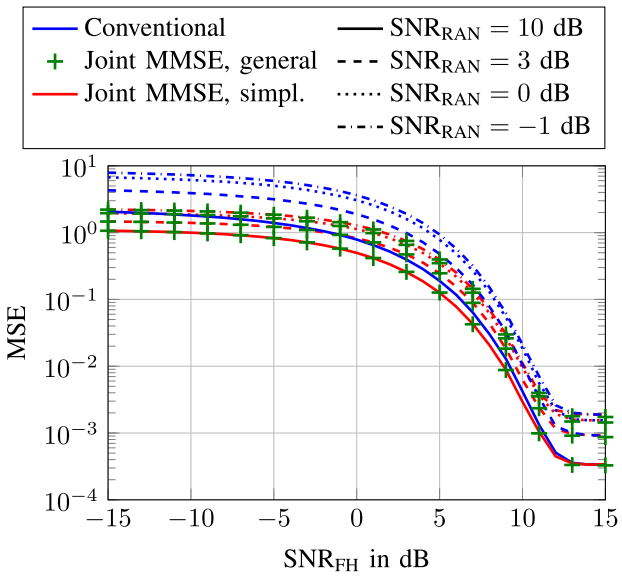

Fig. 7. Mean square error for conventional receiver $\mathrm{E}\left[(x'-\tilde{x})^2\right]$ (blue) and using the proposed MMSE receiver $\mathrm{E}\left[(x'-\hat{x})^2\right]$ in the general (green) and simplified (red) variant for different RAN and FH SNRs.

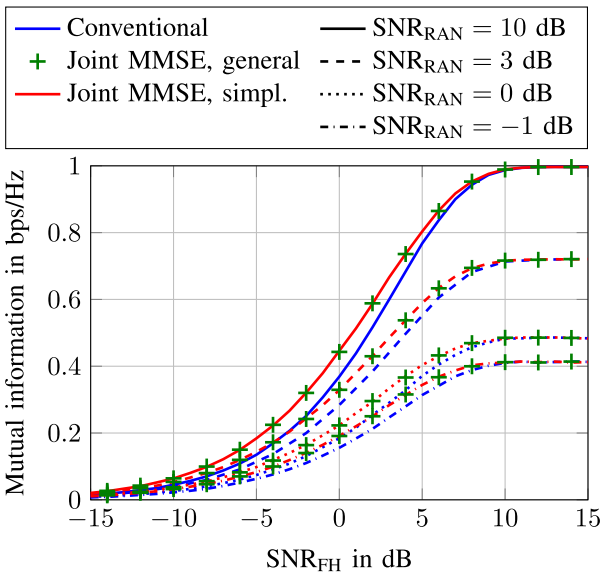

Fig. 8. Mutual information for conventional receiver $I(x;\tilde{x})$ (blue) and using the proposed MMSE receiver $I(x;\hat{x})$ in the general (green) and simplified (red) variant for different RAN and FH SNRs.

performance at a lower $\mathrm{SNR}_{\mathrm{FH}}$. Furthermore, it can be noted that the gain is larger for lower values of $\mathrm{SNR}_{\mathrm{FH}}$, whereas for high values of $\mathrm{SNR}_{\mathrm{FH}}$, the performance of the joint receiver converges to that of the conventional one. This can be expected, as for high values of $\mathrm{SNR}_{\mathrm{FH}}$ the FH is very reliable, and hence there is little difference between the conventional hard decision and the MMSE approach. Furthermore, it can be seen from Fig. 7 that there is only a negligible difference in performance between the simplified receiver with reduced complexity introduced in Sec. III-B, and the general variant in Sec. III-A.

B. Mutual Information

As discussed above, the MSE on the FH is improved as expected. However, the overall aim of the proposed joint receiver is to improve end-to-end communication, i.e. across both RAN and FH channel. In mobile networks, forward error correcting codes (FECs) are utilized to improve end-to-end performance. As the performance depends on the type of code used and the actual implementation, we first investigate the mutual information, which is independent of the FEC used. The end-to-end mutual information for our model is defined as:

$$I(x;\hat{x}) = \sum_{x,\hat{x}} p(x)p(\hat{x}|x)\log_2\left(\frac{p(\hat{x}|x)}{\sum_x p(x)p(\hat{x}|x)}\right). \quad (21)$$

Fig. 8 shows the mutual information for BPSK, $B = 6$ bit, and AWGN channels of different SNRs. As can be seen, the proposed receiver yields gains of up to 1.5 dB. Again, the gains decrease for high values of $\mathrm{SNR}_{\mathrm{FH}}$. Also, the mutual information flattens out for high values of $\mathrm{SNR}_{\mathrm{FH}}$, as for these values it is limited by the RAN channel. For the highest value of $\mathrm{SNR}_{\mathrm{RAN}}$, the mutual information is limited to 1 bps/Hz due to the chosen modulation scheme of BPSK.

It again can be seen that there is only a negligible difference between the simplified receiver and the general variant. Since the variant with reduced complexity is of higher practical relevance, and since it offers good performance both in the FH MSE and the end-to-end mutual information, all other results for the joint receiver in this section are for the simplified variant. We would like to note that small differences in performance were observed for very low quantizer resolutions, e.g. 1 or 2 bits, as in these cases the difference between x' and c_q is large due to the high quantization noise. However, such low resolutions are unrealistic for real-life networks, where resolutions of up to 15 bits are used [12].

C. End-to-End BER

As the mutual information is a theoretic measure, which may not fully reflect the performance in practically implemented systems, we next investigate the end-to-end BER when using an FEC. This will indicate the benefit of our receiver for a data channel, i.e. for transmitting encoded user data. For this, we added an encoder before the RAN modulator and a decoder after the RAN demodulator. The FEC utilized was the turbo code specified for LTE [34], including a rate matching module, which can adapt the code rate by puncturing and repetition. The proposed receiver should be especially beneficial in combination with a turbo decoder, as the latter makes use of soft input.

For comparison, we also include results for a decode-and-forward scheme (DF), in which all baseband processing including decoding is performed at the RRH, and the decoded bits u' are sent over the (unreliable) FH.

Fig. 9 depicts the end-to-end BER for QPSK, a code rate of 1/3, a quantizer resolution of $B = 6$ bits, and an AWGN RAN channel with different values of $\mathrm{SNR}_{\mathrm{RAN}}$. The number of uncoded RAN bits simulated was approximately 10^7. We also assume perfect channel knowledge, i.e. $\hat{H}_F = H_F$, as the channel estimation error is treated separately in Sec. IV-E.

As can be seen in the figure, the proposed receiver performs better than the conventional one for all of values $\mathrm{SNR}_{\mathrm{RAN}}$.

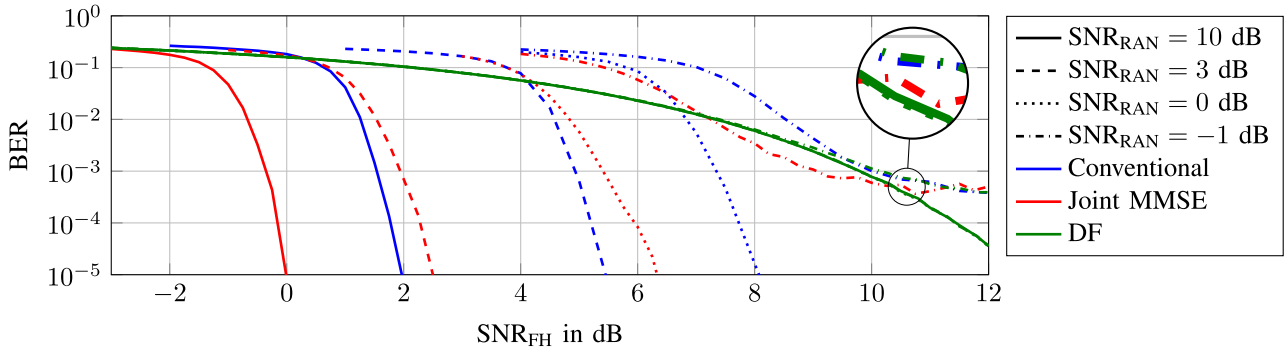

Fig. 9. BER for 4-QAM and AWGN RAN channels with different SNRs. Note that the green lines overlap for the most part.

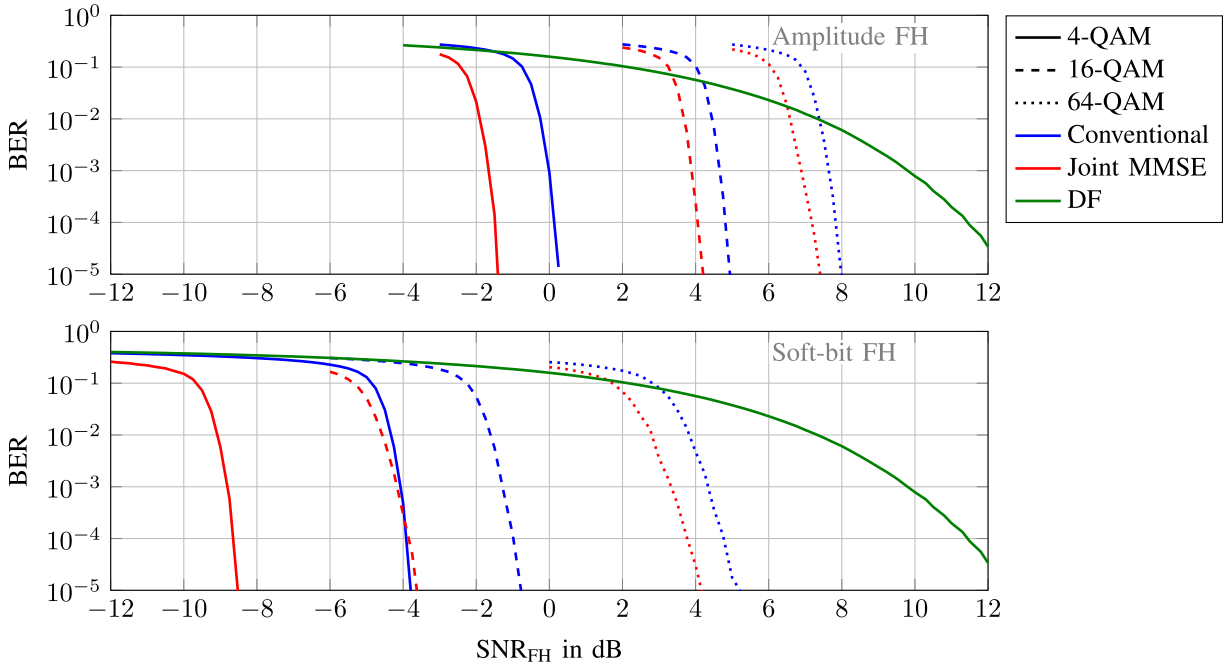

Fig. 10. BER using amplitude fronthauling (top) and soft-bit fronthauling (bottom) for Rayleigh RAN channels, two receive antennas, and different modulation schemes. Note that the green lines overlap.

However, the gain decreases along with $\mathrm{SNR}_{\mathrm{RAN}}$. Similar to the conversion observed in the mutual information, the reason lies in the $\mathrm{SNR}_{\mathrm{FH}}$. For smaller values of $\mathrm{SNR}_{\mathrm{RAN}}$, the waterfall region occurs at a higher $\mathrm{SNR}_{\mathrm{FH}}$. As the improved receiver mitigates the imperfect FH, the benefit of the gets smaller as the $\mathrm{SNR}_{\mathrm{FH}}$ gets large.

Additionally, an error floor is visible for $\mathrm{SNR}_{\mathrm{RAN}} = -1$ dB. In this case, the RAN channel limits the end-to-end performance, such that an increase of $\mathrm{SNR}_{\mathrm{FH}}$ cannot improve performance beyond the RAN channel's limits. A similar error floor can be expected for the other SNRs as well; however, they are too low to be seen from the number of simulated bits. In comparison to the DF-scheme, we observe that the performance of DF depends only on $\mathrm{SNR}_{\mathrm{FH}}$. In fact, the curves correspond to the expected BER of an uncoded 4-QAM transmission. This indicates that the FH is the bottleneck here: all bits can be correctly decoded at the RRH, but new errors are added by the unreliable FH. With the proposed schemes, the data is decoded at the BBU, hence it is still protected on the FH link. For high values of $\mathrm{SNR}_{\mathrm{FH}}$, the RAN becomes again the bottleneck and DF shows a comparable performance.

To further illustrate the benefits of our proposed scheme for different parameters, Fig. 10 shows the BER when using a Rayleigh-fading RAN channel, 2 uncorrelated receive antennas with equal gain combining, the power delay profile of the extended typical urban (ETU) model [35], assuming perfect channel state information (CSI), an $\mathrm{SNR}_{\mathrm{RAN}}$ of 10 dB, and a quantizer resolution of $B = 6$ bits. The top plot shows the BER for a system employing amplitude forwarding, while the bottom plot for utilizing the soft-bit variant. Similar to the AWGN case, considerable gains can be observed for the proposed receiver. The main difference between the amplitude and soft-bit variants is that the overall performance is considerably higher for the soft-bit case, indicating that in general, soft-bit fronthauling can be beneficial in terms of the end-to-end BER.

Finally, Fig. 11 shows the performance increase of the iterative scheme introduced in Sec. III-D for the AWGN RAN.

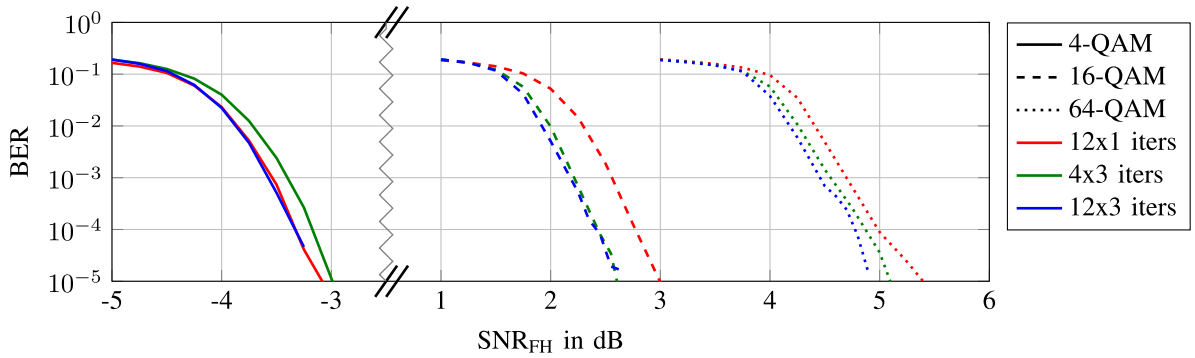

Fig. 11. BER for iterative and non-iterative receiver for AWGN RAN channel.

For this we compare its BER performance for I/Q fronthauling with different modulation schemes, turbo encoding with rate 1/3 and different number of iterations. The number of iterations is given as $a \times b$, with a indicating the number of iterations in the turbo decoder, while b is the number of joint detection iterations. Hence, ax1 indicates the non-iterative scheme with a regular turbo iterations but only one pass through the joint detection step and no feedback. The product $a \cdot b$ indicates the number of total turbo decoder iterations and can be used to fairly compare the complexity of the iterative and non-iterative scheme. As can be seen the joint detection iterations achieve gains of up to 0.4 dB for 4x3 iterations (resulting in a total of 12 turbo decoder iterations) compared to performing 12 regular turbo iterations. An increase to 12x3 (36 decoder iterations) results in an only minimal additional gain. No gains are observed for 4-QAM and in case of 4x3 iterations even a small decrease is in evidence. This is a result of the specific structure of the system. The improvements of the iterative scheme rely on the fact, that correcting a bit error in the decoder impacts on the received amplitude $\hat{x}$ of *another* bit. However, for 4-QAM each bit is mapped to exactly one (I- or Q-) amplitude. Hence a corrected bit error has no impact on other symbols and can hence not correct additional errors in a second decoder pass. As a consequence, the iterative scheme can yield benefits only when utilizing higher-order modulation schemes on the RAN. In addition, we found that again gains can only be observed for high SNR RAN channels in combination with low SNR FH channels.

D. Detection Probability of Synchronization Signals

Apart from user data, the FH also has to transport other forms of RAN signals, e.g. for RAN synchronization or as reference symbols to estimate the RAN channel. As we indicated in the introduction the proposed joint receiver can be applied to arbitrary signals, which we will demonstrate in this section for LTE's physical radio access channel (PRACH).

The main task of the PRACH is to estimate the timing advance of UEs as compared to the BBU. Due to the propagation time of the uplink radio signal, the UEs and BBUs are initially not aligned in time. At the beginning of a transmission, the UEs therefore send a specialized PRACH signal. It is composed of a so-called Zadoff-Chu (ZC) sequence [36], which is family of complex-valued, zero-autocorrelation, constant amplitude sequences. Due to their favorable correlation

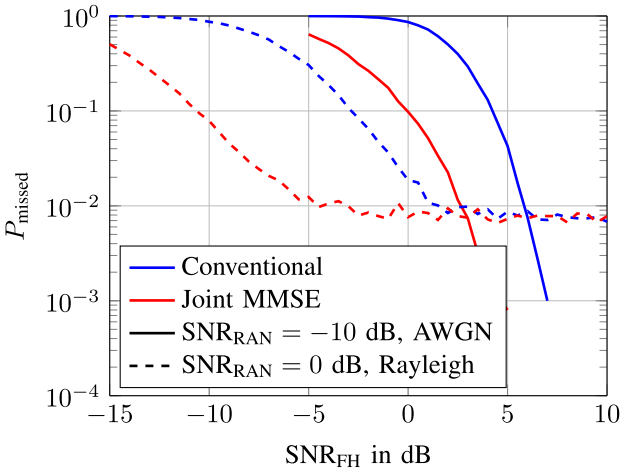

Fig. 12. Missed detection probability for the PRACH using the conventional (blue) and proposed receiver (red) for an AWGN and for a Rayleigh fading channel.

characteristics, they can be used to measure the timing advance of the UE by cross-correlation. A more detail description of the PRACH and timing advance measurement can be found in [37]. The main difference of such a signal compared to the data signals is that it is not chosen from a fixed set of symbols according to a modulation scheme. Instead, it is a sequence of symbols with varying phase. Also, it is not encoded with an FEC, but the shape of the signal is known at the receiver and we merely want to locate the sequence in the noisy received signal. Hence, it has a fundamentally different structure and purpose than a data signal, and we use it to indicate that our proposed receiver is not limited to encoded and modulated signals. In our system model from Fig. 1, the symbols x would now be the ZC-sequence, and the equalizer and RAN demodulator would be replaced by a timing advance estimator.

In general, the PRACH signal first has to be detected by the BBU, for which the correlation peak has to surpass a certain threshold compared to the noise floor. Second, the measured timing advance must be within a certain range of the true timing advance. The requirements of LTE for this are defined in [35]. If the distortion of the signal is too high, the peak will either not be recognized at all, or a wrong peak will be detected, leading to a wrongly estimated timing advance. These events are summarized as a "missed detection". Both the RAN and the FH channel contribute to the distortion of the signal. With the use of the advanced receiver,

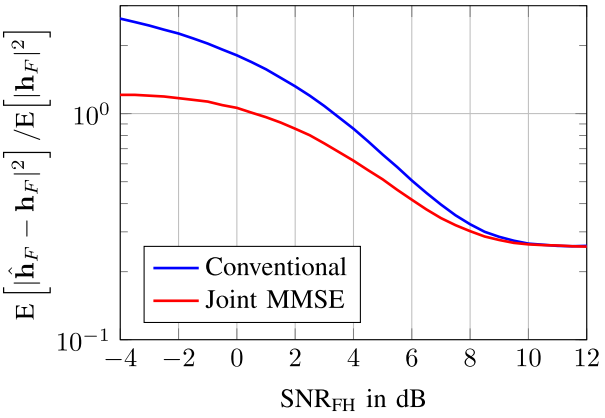

(a) Normalized channel estimation error.

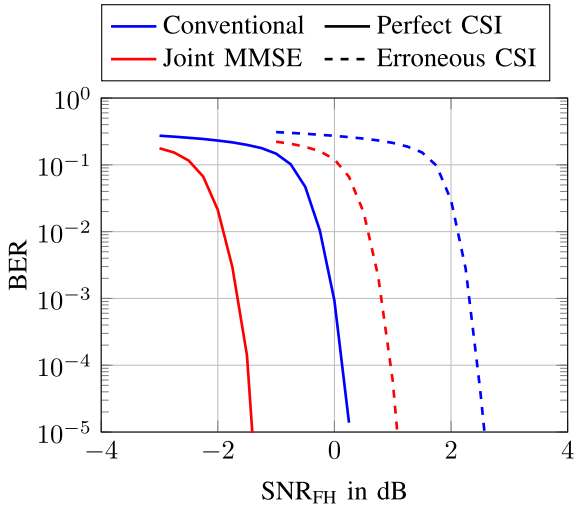

(b) BER comparison for perfect and erroneous channel information.

Fig. 13. Impact of channel estimation error for $\mathrm{SNR}_{\mathrm{RAN}} = 10$ dB.

the distortion of the FH channel can be partly mitigated by performing the MMSE estimation on the amplitudes of the sampled ZC-signal. Fig. 12 shows the probability of a missed detection P_{missed} for the improved as well as for the conventional receiver, using an AWGN RAN channel with $\mathrm{SNR}_{\mathrm{RAN}} = -10$ dB, as well using a Rayleigh channel with $\mathrm{SNR}_{\mathrm{RAN}} = 0$ dB, 270 Hz carrier frequency offset, 70 Hz maximum Doppler frequency and the power delay profile of the ETU channel [35]. Also, for the Rayleigh channel we used two uncorrelated receive antennas with equal gain combining at the receiver and perfect channel knowledge. The quantizer resolution is $B = 6$ bits.

As can be seen from Fig. 12, the joint MMSE receiver achieves a considerable performance gain compared to the conventional one for both channel models. The error floor present for the Rayleigh channel case is a typical effect inherent to the used ZC-sequence in combination with a carrier frequency offset, which is discussed in detail in [38].

E. Impact of Channel Estimation Error

The previous results assumed perfect channel knowledge, i.e. $\hat{H}_F = H_F$. However, if utilizing the amplitude splits,

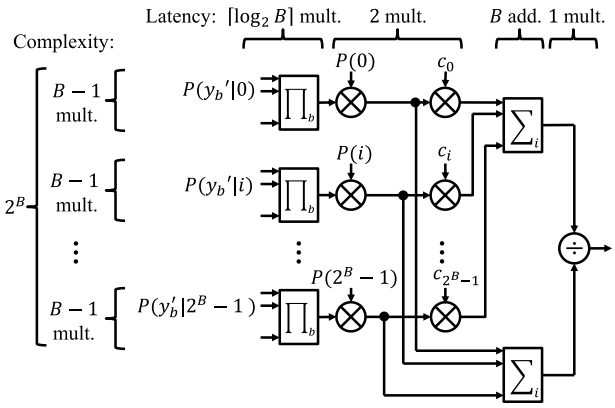

Fig. 14. Hardware architecture for a low-latency implementation of the proposed receiver.

TABLE I
COMPLEXITY OF THE ADVANCED RECEIVER

	Complexity	**Latency**
Add	$2 \cdot (2^B - 1)$	B
Mult	$2^B \cdot (B - 1 + 2) + 1$	$\lceil \log_2(B) \rceil + 3$

the reference signals used for estimation will be quantized and sent through the imperfect FH link along with the data symbols. In the BBU, the reference symbols will be utilized for channel estimation according to Eq. (5). Since the reference symbols are subject to the FH errors, the channel estimation will be erroneous as well. However, the joint receiver will also partially mitigate the FH errors, as the reference symbols can be processed in the same fashion as data symbols according to Eq. (17). Fig. 13a shows the normalized channel estimation error both for utilizing the conventional and joint MMSE receivers. The figure illustrates that in general an imperfect FH increases the channel estimation error; yet the error is lower when utilizing the joint MMSE receiver. Fig. 13b shows the impact of the imperfectly estimated channel on the overall BER performance in comparison with the case of perfect channel knowledge. As can be seen the channel estimation error reduces performance for both the case of the conventional and the joint receiver. However, the joint receiver still provides a gain, as it is beneficial both for the transmission of reference symbols and for data symbols. As the gain is almost equal in both cases, we can deduce that in the given operating range, the errors on the user data caused by the FH are the limiting factor over the channel estimation error.

V. COMPLEXITY

The proposed joint receiver requires additional processing as compared to the conventional hard-decision receiver. A higher computational complexity is of disadvantage as it increases energy consumption and latency. Since the proposed receiver is located in the BBU, energy consumption is less critical than it would be in mobile devices due to their limited power supply by batteries. Latency, however, is very critical because C-RAN puts tight constraints on the maximum latency introduced by FH, as we indicated in the introduction.

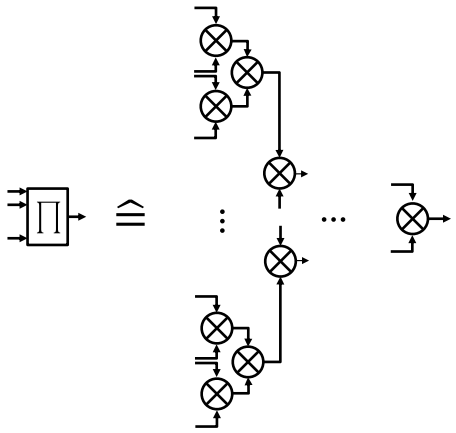

(a) Detailed hardware architecture for product and sum blocks from Fig. 14.

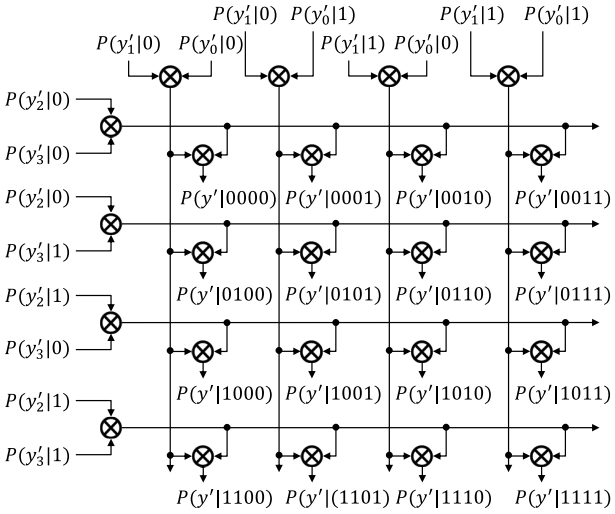

(b) Optimized product block from Fig. 14 for $B = 4$ bits.

Fig. 15. Details of the hardware architecture.

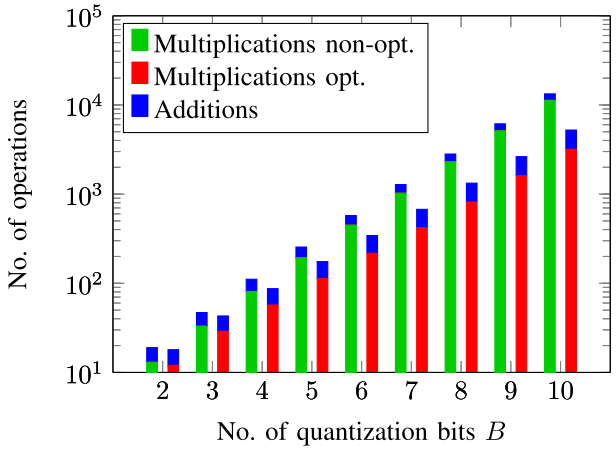

Fig. 16. Computational complexity in number of multiplications and additions for the non-optimized (green) and optimized (red) architecture.

In Table I, we summarized both the complexity and the latency in terms of floating point additions and multiplications to calculate Eq. (17). We did not include the calculation of the input probabilities $p(y_b|i_b)$ and $p(i)$, as the former is also required for the conventional receiver and the latter can be simply measured as discussed in Sec. III. The considered hardware architecture is depicted in Fig. 14, with a detailed view of the product and sum blocks depicted in Fig. 15a. The complexity is exponential in B; however, the more critical latency is only linear/ logarithmic in B, meaning that even for high resolution quantizers, the calculations can be performed in short time. The low latency can be achieved, since most of the operations can be performed in parallel at the cost of a higher hardware complexity.

To further reduce the complexity, it is possible to reuse results within the product blocks calculating all possible $p(y'|i)$, which is shown for $B = 4$ bits in Fig. 15b. The complexity here is only 24 multiplications (compared to 48 in Fig. 15a) at the same latency of 2 multiplications. Similar optimization can be done for all numbers of B. The results are illustrated in Fig. 16, which shows the total number of additions and multiplication for the optimized and not optimized case. As can be seen, the number of multiplications is reduced by up to 70 % (note the logarithmic scale) by this optimization.

The iterative scheme in Sec. III-D scales the latency with the number of iterations and adds complexity in terms of the feedback loop. However, since it offers only a small performance gain, the non-iterative variant seems the more efficient choice.

VI. Conclusion

FH links are an integral part of any C-RAN system. However, in current approaches, RAN and FH signals are processed separately, thereby requiring the FH to be nearly error-free in order to not impact performance. Accordingly, the current systems are not designed to deal with unreliable FH technologies like mmWave wireless links, yet those could enable more cost-efficient deployments. In this work, we have shown how to deal with a reduced FH reliability by a joint design of access and fronthaul. For this, we have developed a joint RAN/ FH receiver that performs MMSE estimation utilizing both soft information from the FH link as well as statistical information of the RAN signal in order to improve end-to-end performance. This receiver can be applied to arbitrary signals, including user data transmission using either amplitude-based or soft-bit based fronthauling, synchronization signal, or reference signal fronthauling. For all use cases the proposed joint receiver offers an improved performance over the conventional hard-decision implementation. The performance gain depends on the fronthaul channel's quality and is especially pronounced when the FH channel exhibits a low SNR. Hence, it is most suitable for wireless FH links which suffer from reduced reliability as compared to fiber. As the proposed receiver increases the computational complexity compared to the conventional approach, we have developed a simplified version, which can be implemented highly parallel, ensuring a low latency, which is critical in context of cloud radio access networks. An iterative extension of the proposed receiver can be beneficial in case of an AWGN RAN channel and higher order modulation schemes.

In summary, the proposed receiver not only promises an improved performance in theory, but with our investigation of relevant applications and on how to handle the increased complexity, we are confident that it can also be implemented in practice.

APPENDIX
PROBABILITY DISTRIBUTIONS

The proposed receiver utilizes the conditional probabilities $p(x'|x)$ to calculate the MMSE estimator. In this appendix we give the required distributions and integrals for the AWGN and Rayleigh RAN case, as well as for soft-bit fronthauling.

A. Amplitude Forwarding and AWGN RAN Channel

For BPSK and AWGN channels on both the RAN and FH we have the channel transition probabilities:

$$p(x'|x=\pm 1) = \frac{1}{\sqrt{2\pi\,\sigma^2_{RAN}}} \exp\left(-\frac{(\pm 1 - x')^2}{2\sigma^2_{RAN}}\right), \quad (22)$$

and

$$p(y'_b|i_b = \tfrac{1}{0}) = \frac{1}{\sqrt{2\pi\,\sigma^2_{FH}}} \exp\left(-\frac{(\pm 1 - y'_b)^2}{2\sigma^2_{FH}}\right), \quad (23)$$

where $i_b = \frac{1}{0}$ denotes the two cases of i_b being either one or zero.

The general MMSE estimator was given in Eq. (13) as:

$$\hat{x} = \frac{\int_{x'} x' \sum_x p(x)\, p(x'|x) \prod_b p(y'_b|q_b(x'))\, dx'}{\int_{x'} \sum_x p(x)\, p(x'|x) \prod_b p(y'_b|q_b(x'))\, dx'}, \quad (24)$$

where we have now written $q_b(x')$ to indicate that q_b is a function of x'. Within the decision thresholds of a given index i, we have $q_b(x') = i_b \,\forall\, x' \in [t_i, t_{i+1}]$. Hence, we can reformulate the integral as a sum of integrals over the decision regions:

$$\hat{x} = \frac{\sum_{i\in I} \sum_x p(x) \prod_b p(y'_b|i_b) \int_{t_i}^{t_{i+1}} x' p(x'|x)\, dx'}{\sum_{i\in I} \sum_x p(x) \prod_b p(y'_b|i_b) \int_{t_i}^{t_{i+1}} p(x'|x)\, dx'} \quad (25)$$

The integral in the nominator of Eq. (25) is given as:

$$\int_{t_i}^{t_{i+1}} x' p(x'|x=\pm 1)\, dx' = \frac{1}{2}\Bigg[\mp \operatorname{erfc}\left(\frac{x'-1}{\sqrt{2\sigma^2_{RAN}}}\right) - \sqrt{\frac{2\sigma^2_{RAN}}{\pi}} \exp\left(-\frac{(\pm 1 - x')^2}{2\sigma^2_{RAN}}\right)\Bigg]_{t_i}^{t_{i+1}} \quad (26)$$

The integrals in the denominator of Eq. (25) as well as for Eq. (18) are given as:

$$\int_{t_i}^{t_{i+1}} p(x'|x=\pm 1)\, dx' = \left[\frac{1}{2} \operatorname{erfc}\left(\frac{x' \pm 1}{\sqrt{2\sigma^2_{RAN}}}\right)\right]_{t_i}^{t_{i+1}} \quad (27)$$

B. Amplitude Forwarding and Rayleigh RAN Channel

For the single-tap Rayleigh fading channel without ISI we have

$$\begin{aligned} x' &= hx + n && (28)\\ &= (h_R + jh_I)(x_R + jx_I) + n_R + n_I && (29)\\ &= h_R x_R - h_I x_I + n_R + j(h_I x_R + h_R x_I + n_I) && (30)\end{aligned}$$

with subscripts R and I denoting the real and imaginary parts. Since h_R, h_I, n_R, and n_I are all Gaussian distributed with zero mean, the resulting distribution in I-phase can easily be shown to be

$$p(x'|x) = \frac{1}{\sqrt{2\pi\,\sigma^2_{\text{ray}}}} \exp\left(-\frac{x'^2}{2\sigma^2_{\text{ray}}}\right) \quad (31)$$

with

$$\sigma^2_{\text{ray}} = |x_R|^2\sigma^2_{\text{h}} + |x_I|^2\sigma^2_{\text{h}} + \sigma^2_{RAN}. \quad (32)$$

From this, we have the integral required for Eq. (18) for the Rayleigh case:

$$\int_{t_i}^{t_{i+1}} p(x'|x)\, dx' = \frac{1}{2}\left[\operatorname{erfc}\left(\frac{x'}{2\sigma_{\text{ray}}}\right)\right]_{t_{i+1}}^{t_i} \quad (33)$$

C. Soft-Bit Forwarding

For the soft-bit case, the integral for Eq. (20) is given as [39]:

$$\begin{aligned}\int_{t_i}^{t_{i+1}} p(\lambda'|x=\pm 1)\, d\lambda &= \int_{t_i}^{t_{i+1}} \frac{1}{(1-\lambda^2)\sqrt{2\pi\,\sigma^2_\lambda}} \\ &\quad \times\left[\exp\left(-\frac{(2\operatorname{artanh}(\lambda) \mp \sigma^2_\lambda)^2}{2\sigma^2_\lambda}\right)\right] d\lambda && (34)\\ &= -\frac{1}{2}\left[\operatorname{erfc}\left(\frac{2\operatorname{artanh}(\lambda) - \sigma^2_\lambda}{\sqrt{2\sigma^2_\lambda}}\right)\right]_{t_i}^{t_{i+1}}, && (35)\end{aligned}$$

with $\sigma^2_\lambda = 4/\sigma^2_{RAN}$.

REFERENCES

[1] H. Guan, T. Kolding, and P. Merz, "Discovery of cloud-RAN," in *Proc. Cloud-RAN Workshop*, Apr. 2010, pp. 1–13.

[2] C.-L. I., J. Huang, R. Duan, C. Cui, J. Jiang, and L. Li, "Recent progress on C-RAN centralization and cloudification," *IEEE Access*, vol. 2, pp. 1030–1039, 2014.

[3] P. Rost *et al.*, "Cloud technologies for flexible 5G radio access networks," *IEEE Commun. Mag.*, vol. 52, no. 5, pp. 68–76, May 2014.

[4] A. Checko *et al.*, "Cloud ran for mobile networks—A technology overview," *IEEE Commun. Surveys Tuts.*, vol. 17, no. 1, pp. 405–426, 1st Quart., 2015.

[5] R. Irmer *et al.*, "Coordinated multipoint: Concepts, performance, and field trial results," *IEEE Commun. Mag.*, vol. 49, no. 2, pp. 102–111, Feb. 2011.

[6] CPRI. *Common Public Radio Interface (CPRI)*. Access on Jan. 6, 2017. [Online]. Available: http://www.cpri.info/

[7] B. Guo, W. Cao, A. Tao, and D. Samardzija, "LTE/LTE-A signal compression on the CPRI interface," *Bell Labs Tech. J.*, vol. 18, no. 2, pp. 117–133, Sep. 2013.

[8] J. Lorca and L. Cucala, "Lossless compression technique for the fronthaul of LTE/LTE-advanced cloud-RAN architectures," in *Proc. IEEE 14th Int. Symp. Workshops World Wireless, Mobile Multimedia Netw. (WoWMoM)*, Jun. 2013, pp. 1–9.

[9] S. Nanba and A. Agata, "A new IQ data compression scheme for front-haul link in centralized RAN," in *Proc. IEEE 24th Int. Symp. Pers., Indoor Mobile Radio Commun. (PIMRC Workshops)*, Sep. 2013, pp. 210–214.

[10] S.-H. Park, O. Simeone, O. Sahin, and S. Shamai (Shitz), "Fronthaul compression for cloud radio access networks: Signal processing advances inspired by network information theory," *IEEE Signal Process. Mag.*, vol. 31, no. 6, pp. 69–79, Nov. 2014.

[11] Y. Zhou and W. Yu, "Fronthaul compression and transmit beamforming optimization for multi-antenna uplink C-RAN," *IEEE Trans. Signal Process.*, vol. 64, no. 16, pp. 4138–4151, Aug. 2016.

[12] U. Dötsch, M. Doll, H. P. Mayer, F. Schaich, J. Segel, and P. Sehier, "Quantitative analysis of split base station processing and determination of advantageous architectures for LTE," *Bell Labs Tech. J.*, vol. 18, no. 1, pp. 105–128, May 2013.

[13] D. Sabella *et al.*, "Ran as a service: Challenges of designing a flexible ran architecture in a cloud-based heterogeneous mobile network," in *Proc. Future Netw. Mobile Summit (FuNeMS)*, Lisbon, Portugal, Jul. 2013, pp. 1–8.

[14] J. Huang *et al.*, "White paper of next generation fronthaul interface," China Mobile Res. Inst., Beijing, China, White Paper, Jun. 2015, accessed on Oct. 20, 2015. [Online]. Available: http://labs.chinamobile.com/cran/wp-content/uploads/White%20Paper%20of%20Next%20Generation%20Fronthaul%20Interface.PDF

[15] J. Bartelt, P. Rost, D. Wubben, J. Lessmann, B. Melis, and G. Fettweis, "Fronthaul and backhaul requirements of flexibly centralized radio access networks," *IEEE Wireless Commun.*, vol. 22, no. 5, pp. 105–111, Oct. 2015.

[16] C. L. I., Y. Yuan, J. Huang, S. Ma, C. Cui, and R. Duan, "Rethink fronthaul for soft RAN," *IEEE Commun. Mag.*, vol. 53, no. 9, pp. 82–88, Sep. 2015.

[17] *Standard for Packet-Based Fronthaul Transport Networks*, IEEE Standard P1914.1. accessed on 2016. [Online]. Available: https://standards.ieee.org/develop/project/1914.1.html/

[18] "Microwave towards 2020," Ericsson, Stockholm, Sweden, White Paper, Sep. 2015, accessed on Oct. 20, 2015. [Online]. Available: http://www.ericsson.com/res/docs/2015/microwave-2020-report.pdf

[19] M. Peng, C. Wang, V. Lau, and H. V. Poor, "Fronthaul-constrained cloud radio access networks: Insights and challenges," *IEEE Wireless Commun.*, vol. 22, no. 2, pp. 152–160, Apr. 2015.

[20] "Buisness case elements for small cell virtualization," Real Wireless Ltd., Pulborough, U.K., White Paper SCF 158, Jun. 2015, accessed on Oct. 20, 2015. [Online]. Available: http://scf.io/en/documents/158_-_Business_case_elements_for_small_cell_virtualization.php

[21] M. Marcus and B. Pattan, "Millimeter wave propagation: Spectrum management implications," *IEEE Microw. Mag.*, vol. 6, no. 2, pp. 54–62, Jun. 1997.

[22] J. Bartelt and G. Fettweis, "A soft-input/soft-output dequantizer for cloud-based mobile networks," in *Proc. IEEE 15th Int. Workshop Signal Process. Adv. Wireless Commun. (SPAWC)*, Jun. 2014, pp. 404–408.

[23] J. Bartelt and G. Fettweis, "An improved decoder for cloud-based mobile networks under imperfect fronthaul," in *Proc. Globecom Workshop-Wireless Opt. Netw. Converg. Support Cloud Archit. (GC WS-WONC)*, Austin, TX, USA, Dec. 2014, pp. 1499–1504.

[24] J. Bartelt, L. Landau, and G. Fettweis, "Improved uplink I/Q-signal forwarding for cloud-based radio access networks with millimeter wave fronthaul," in *Proc. IEEE 12th Int. Symp. Wireless Commun. Syst.*, Brussels, Belgium, Aug. 2015, pp. 341–345.

[25] M. R. Souryal and H. You, "Quantize-and-forward relaying with M-ARY phase shift keying," in *Proc. IEEE Wireless Commun. Netw. Conf.*, Mar. 2008, pp. 42–47.

[26] B. Djeumou, S. Lasaulce, and A. G. Klein, "Practical quantize-and-forward schemes for the frequency division relay channel," *EURASIP J. Wireless Commun. Netw.*, vol. 2007, pp. 2:1–2:11, Oct. 2007. [Online]. Available: http://dx.doi.org/10.1155/2007/20258

[27] I. Avram, N. Aerts, H. Bruneel, and M. Moeneclaey, "Quantize and forward cooperative communication: Channel parameter estimation," *IEEE Trans. Wireless Commun.*, vol. 11, no. 3, pp. 1167–1179, Mar. 2012.

[28] J. Max, "Quantizing for minimum distortion," *IRE Trans. Inf. Theory*, vol. 6, no. 1, pp. 7–12, Mar. 1960.

[29] S. Lloyd, "Least squares quantization in PCM," *IEEE Trans. Inf. Theory*, vol. 28, no. 2, pp. 129–137, Mar. 1982.

[30] S. M. Kay, "General Bayesian estimators," in *Fundamentals Statistical Processin: Estimation Theory*, vol. 1. Upper Saddle River, NJ, USA: Prentice-Hall, 1993, ch. 11, pp. 341–375.

[31] S. Benedetto, D. Divsalar, G. Montorsi, and F. Pollara, "A soft-input soft-output maximum a posteriori MAP module to decode parallel and serial concatenated codes," *TDA Prog. Rep.*, vol. 42, no. 127, pp. 1–20, 1996.

[32] M. Springer and W. Thompson, "The distribution of products of independent random variables," *SIAM J. Appl. Math.*, vol. 14, no. 3, pp. 511–526, 1966.

[33] Z. Lomnicki, "On the distribution of products of random variables," *J. Roy. Statist. Soc. B (Methodol.)*, vol. 29, no. 3, pp. 513–524, 1967.

[34] *LTE; Evolved Universal Terrestrial Radio Access (E-UTRA); Multiplexing and Channel Coding 3GPP Std.*, document 3GPP TS 36.212, Apr. 2013.

[35] *LTE; Evolved Universal Terrestrial Radio Access (E-UTRA); Base Statio (BS) Conformance Testing 3GPP Std.*, document 3GPP TS 36.141, Jan. 2011.

[36] D. Chu, "Polyphase codes with good periodic correlation properties (Corresp.)," *IEEE Trans. Inf. Theory*, vol. 18, no. 4, pp. 531–532, Jul. 1972.

[37] S. Stefania, T. Issam, and B. Matthew, *LTE, the UMTS Long Term Evolution: From Theory to Practice*. Sussex, U.K.: Wiley, 2009, ch. 19.

[38] M. Hua, M. Wang, K. Yang, and K. Zou, "Analysis of the frequency offset effect on Zadoff–Chu sequence timing performance," *IEEE Trans. Commun.*, vol. 62, no. 11, pp. 4024–4039, Nov. 2014.

[39] S. Khattak, W. Rave, and G. Fettweis, "Distributed iterative multi-user detection through base station cooperation," *EURASIP J. Wireless Commun. Netw.*, vol. 2008, pp. 1–15, Jan. 2008.

Jens Bartelt received the Dipl.Ing. (MSEE) degree from Technische Universität Dresden, Germany, in 2012, where he is currently pursuing the Ph.D. degree. From 2011 to 2012 he was an Intern with Rohde & Schwarz, Munich. Since 2013, he has been a Research Associate with Vodafone Chair Mobile Communications Systems, Technische Universität Dresden. He is currently involved in several 5G research activities, including the EU projects iJOIN and 5G-XHaul, and the 5G Lab Germany, Technische Universität Dresden. His research interests include cloud-based mobile networks, mm-wave communication, and physical-layer signal processing.

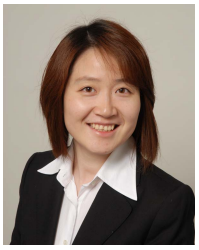

Dan Zhang received the B.Sc. degree in electrical engineering from Zhejiang University, China, in 2004, and the M.Sc. and Dr. Ing. degrees in electrical engineering and information technology from RWTH Aachen University, Aachen, Germany, in 2007 and 2013, respectively. During her Ph.D. studies, she focused on iterative receiver designs. Since 2014, she has been a Post-Doctoral Researcher with Vodafone Chair Mobile Communications Systems, Technische Universität Dresden. She has focused on various national and international research projects with publication in journals, conference proceedings, and workshops. Her current research focus is on the transceiver design of multicarrier waveforms with the objective of providing a new air interface for 5G networks. Her research interests include statistical signal processing, communication theory, and optimization theory.

Gerhard Fettweis (S'84–M'90–SM–98'F'09) received the Dipl.Ing. and Ph.D. degrees from RWTH Aachen University, Germany, and the Ph.D. degree (Hons.) from Tampere University, in 2012. From 1990 to 1991, he was a Visiting Scientist with the IBM Almaden Research Center, San Jose, CA, USA, where he was involved in signal processing for disk drives. From 1991 to 1994, he was with TCSI Inc., Berkeley, CA, USA, responsible for signal processor developments. Since 1994, he has been the Vodafone Chair with Technische Universität Dresden, Germany. He is also a well-known serial entrepreneur who has co-founded 11 start-ups to date. He has been an elected member of the IEEE Solid State Circuits Societies Board (Administrative Committee) since 1999, and he is also an elected member of the IEEE Fellow Committee. He also coordinates two DFG centers at Technische Universität Dresden, namely, Highly Adaptive Energy Efficient Computing and Center for Advancing Electronics Dresden.